

SPHERE: Spherical partitioning for large-scale routing optimization

Robert Fabian Lindermann¹ Paul-Niklas Ken Kandora¹ Simon Caspar Zeller¹

Adrian Asmund Fessler¹

¹Institute for Operations Research, Karlsruhe Institute of Technology, Karlsruhe, Germany
 {paul-niklas.kandora, simon.zeller, steffen.rebennack}@kit.edu
 {robert.lindermann, adrian.fessler}@student.kit.edu

Abstract

We study shortest-path routing in large weighted, undirected graphs, where expanding search frontiers raise time and memory costs for exact solvers. We propose *SPHERE*, a source-target-aware heuristic that identifies an s - t overlap: vertices that are close to both s and t in hop count. Selecting an anchor a in this overlap partitions the task into two subproblems with unchanged problem-topology, $s \rightarrow a$ and $a \rightarrow t$; if either remains large, the procedure recurses on its induced subgraph. Because the cut lies inside the overlap, concatenating the resulting subpaths yields a valid $s \rightarrow t$ route without boundary repair. *SPHERE* is independent of the downstream solver (e.g., Dijkstra) and exposes parallelism across subproblems. On large networks, it achieves faster runtimes and smaller optimality gaps than Louvain-based routing and a METIS-based pipeline, even on graphs with more than a million nodes and edges, while also outperforming Dijkstra in runtime.

1 Introduction

Point-to-point routing in large weighted, undirected graphs is a canonical problem in operations research, one that emerged alongside the field's inception.. Exact label-setting or label-correcting methods (e.g., Dijkstra) can certify optimality (Dijkstra, 1959), but

their search frontiers grow quickly on large networks and become memory- and time-intensive. Graph partitioning methods (e.g., Kernighan-Lin, multilevel partitioning/METIS, spectral cuts) reduce problem size by cutting the graph into parts (Kernighan and Lin, 1970; Karypis and Kumar, 1998; Shi and Malik, 2000), yet cuts chosen without regard to a specific query (s, t) can intersect narrow passages that many feasible s - t routes must use, which can exclude high-quality routes or require costly boundary repair. Bidirectional search reduces depth by growing frontiers from s and t (Nicholson, 1966; Pohl, 1969; Kaindl and Kainz, 1997; Holte et al., 2016), but still explores a single coupled state space and may expand many partial routes on large graphs. For completeness, we note that while feasibility for unconstrained shortest paths is trivial on connected graphs, constrained variants (e.g., resource- or budget-limited paths) are NP-hard; our focus here is the unconstrained case with nonnegative weights, which admits an optimal solution via Dijkstra's algorithm (Dijkstra, 1959).

We propose *SPHERE*, a query-aware partition that aligns computation to the s - t geometry. Let $B_s(r)$ and $B_t(r)$ denote *hop-distance spheres* around s and t . *SPHERE* starts from a radius tuple (r_s, r_t) with guaranteed overlap $B_s(r_s) \cap B_t(r_t) \neq \emptyset$, then applies a monotone *decrement* rule that reduces the radii (when needed, both simultaneously) so that $|r_s - r_t| \leq 1$ while preserving overlap, and selects the *minimal balanced* pair, i.e. no further admissible unit decrement of either radius (still keeping $|r_s - r_t| \leq 1$) leaves the intersection nonempty. Then it selects an anchor $a \in B_s(r_s) \cap B_t(r_t)$ and splits the query into

$s \rightarrow a$ and $a \rightarrow t$, solved on the corresponding induced subgraphs under a tunable size cap. If a subproblem still exceeds the cap, the procedure recurses on its induced subgraph. Because the cut lies inside the overlap, concatenating subpaths at a yields a valid $s-t$ route without boundary repair. The partition is solver-agnostic and the independent subproblems can be solved in parallel.

Our contributions are:

1. **Query-aware partition.** We introduce a simple heuristic that adaptively splits the graph based on the geometry of the source-target pair, ensuring that each part preserves connectivity and can be rejoined without additional repair.
2. **Parallel subinstances.** The subproblems generated by SPHERE are independent induced subgraphs, naturally exposing parallelism and enabling scalable routing on distributed systems with effort scaling to hardware.
3. **Empirical validation.** On large road graphs, SPHERE achieves faster runtimes than Louvain-based routing and a METIS-based pipeline while matching or improving route quality, benefiting further from inherent parallelism.

SPHERE is complementary to downstream solvers and can wrap Dijkstra or A* (Dijkstra, 1959; Hart et al., 1968), as well as modern speedup indices such as ALT/landmarks (Goldberg and Harrelson, 2005), reach-based pruning (Gutman, 2004), contraction hierarchies (Geisberger et al., 2008), hub labeling (Abraham et al., 2011), and transit-node routing (Bast et al., 2016); we evaluate with common solvers and baselines and discuss integration in Section 5. Next, we motivate these design choices by examining where existing approaches trade-off feasibility, and instance size, before positioning SPHERE within the literature and formalizing our approach.

2 Motivation

Routing at scale must meet three criteria simultaneously: control per-instance complexity, make an $s-t$ route feasible, and remain compatible with trusted downstream solvers while enabling parallel execution. Existing tools typically sacrifice at least one of these: Labeling methods (Feillet et al., 2004; Irnich and Desaulniers, 2005) preserve feasibility but

generate a combinatorial explosion of partial routes on large graphs. Graph partitioners (Kernighan and Lin, 1970; Karypis and Kumar, 1998; Shi and Malik, 2000) control instance size, but because their boundaries are chosen without regard to s and t , they may cut across a bottleneck that every feasible $s-t$ path must traverse, risking the loss of valid routes. Bidirectional search (Nicholson, 1966; Pohl, 1969; Kaindl and Kainz, 1997; Holte et al., 2016) reduces search depth by expanding from both ends, s and t , but the two frontiers still form a single combined search space and therefore cannot be partitioned into smaller, independent pieces suitable for parallel solution.

SPHERE overcomes these trade-offs by aligning the partition with the specific request. To ensure controllable size, it expands hop-distance spheres from s and t until reaching the last nonempty overlap, where a user-defined radius limits the diameter of each subproblem. Second, for feasibility, SPHERE selects an anchor a in the overlap and solves $s \rightarrow a$ and $a \rightarrow t$ on their respective induced subgraphs, so cuts always lie inside the overlap and concatenation at a is guaranteed to generate a feasible $s-t$ route. This preserves all local connectivity within each part and ensures that every feasible subpath remains feasible in the global graph. Third, the resulting subproblems are independent, enabling parallel execution across multiple cores, and the design is solver-agnostic which means that any downstream optimizer, from exact *Mixed-Integer Programming (MIP)* on small pieces to strong metaheuristics on larger ones (Pisinger and Ropke, 2007; Vidal, 2022), can be applied without modification. In short, SPHERE offers a partition strategy that controls complexity, preserves feasibility, and exposes natural parallelism while remaining compatible with the solvers practitioners already trust.

3 Related Work

Point-to-point routing on large weighted graphs has been studied from several perspectives. Classical exact methods such as label-setting and label-correcting algorithms (e.g., Dijkstra) can guarantee global optimality on connected graphs with nonnegative weights (Dijkstra, 1959). Dynamic-programming and labeling variants extend this to richer settings and can certify optimality, but they often face an explosion in the number of labels on large graphs (Feillet et al., 2004; Irnich and Desaulniers, 2005). Approximation schemes exist for restricted variants (Hassin, 1992),

trading accuracy for speed, yet these techniques operate on the full graph and therefore do not reduce the instance size before optimization.

Graph partitioning offers a complementary idea: simplify the problem by splitting the graph. Kernighan-Lin improves an initial cut by greedy node swaps to reduce the number of edges crossing between parts while keeping parts balanced (Kernighan and Lin, 1970). Multilevel schemes such as METIS repeatedly coarsen the graph, compute a cut on the coarse instance, and refine it during uncoarsening, which gives strong scalability in practice (Karypis and Kumar, 1998). In routing pipelines, these partitions are often used to build a quotient graph for a coarse path that is later refined within parts. A limitation of all such methods is that the cut is chosen without regard to the specific start-target pair (s, t) , so the boundary can lie across a narrow passage that every feasible $s-t$ path must use. Once this happens, the coarse or restricted routing stage may miss or degrade the necessary connection.

Bidirectional search reduces search depth by expanding frontiers from both ends and meeting near the middle (Nicholson, 1966; Pohl, 1969; Kaindl and Kainz, 1997). The MM algorithm of Holte et al. (2016) provides a priority rule that ensures expansions do not go beyond the midpoint of the optimal solution. These methods improve exploration efficiency but still operate within a single coupled search space and do not produce small, independent instances. In large graphs this can still generate many partial routes, and unlike partition-based methods, they do not offer a straightforward path to parallel, solver-agnostic execution.

4 Spherical Partitioning

4.1 Spherical subgraphs

We begin by fixing distance and the local “window” around a node. In the following, let every graph $G = (V, E)$ be a finite, connected, undirected graph with positive edge weights. Unless stated otherwise we measure distance in hops (unweighted shortest path); all statements below remain valid for the weighted shortest-path distance.

Definition 1 (Spheres). *For $R \in \mathbb{N}$ and a reference node $\tilde{v} \in V$, the (closed) sphere is*

$$S_R(\tilde{v}) := \{v \in V : d_G(\tilde{v}, v) \leq R\} \subseteq V,$$

where $d_G(\tilde{v}, v)$ is the unweighted shortest path dis-

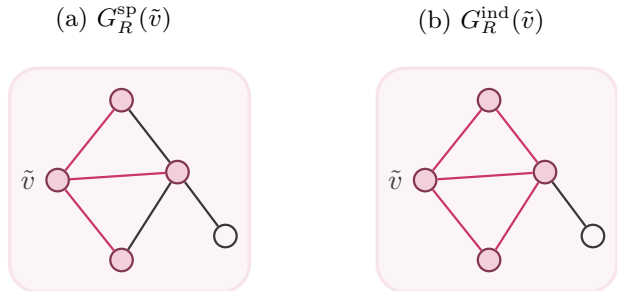


Figure 1: **Two local views on $S_R(\tilde{v})$.** Left: keep edges on shortest paths to \tilde{v} . Right: keep all edges among nodes in the sphere (induced).

tance between \tilde{v} and v .

Two standard subgraphs provide complementary local views of G on the node set $S_R(\tilde{v})$.

Definition 2 (Spherical subgraph). $G_R^{sp}(\tilde{v}) := (V_R(\tilde{v}), E_R^{sp}(\tilde{v}))$ with $V_R(\tilde{v}) = S_R(\tilde{v})$ and

$$E_R^{sp}(\tilde{v}) = \bigcup_{v \in S_R(\tilde{v})} \mathcal{E}(\text{SP}(\tilde{v}, v)),$$

the union of edges along some shortest $\tilde{v}-v$ path for each $v \in S_R(\tilde{v})$.

Definition 3 (Induced spherical subgraph). $G_R^{ind}(\tilde{v}) := (V_R(\tilde{v}), E_R^{ind}(\tilde{v}))$ with $V_R(\tilde{v}) = S_R(\tilde{v})$ and

$$E_R^{ind}(\tilde{v}) = \{(i, j) \in E : i, j \in S_R(\tilde{v})\}.$$

Clearly $E_R^{sp}(\tilde{v}) \subseteq E_R^{ind}(\tilde{v})$: the spherical subgraph preserves shortest-path connectivity to the center, while the induced version preserves all *local* connectivity.

4.2 Partition cut

With these building blocks in place, we now align the local windows to a specific query (s, t) . For radii $(R_s, R_t) \in \mathbb{N}^2$, define the *overlap*

$$O(R_s, R_t) := S_{R_s}(s) \cap S_{R_t}(t).$$

We control how radii evolve, how they are initialized, and how an anchor is chosen in the overlap.

Definition 4 (Decrement rule). *A decrement rule is a map $\text{decr} : \mathbb{N}^2 \rightarrow \mathbb{N}^2$ that is monotone in the lexicographic order, i.e.,*

$$(x_1, x_2) \leq_{\text{lex}} (y_1, y_2) \iff x_1 < y_1, \quad \text{or } (x_1 = y_1 \text{ and } x_2 \leq y_2).$$

and never increases any coordinate.

Example (monotone decrement). A simple rule that satisfies the definition is

$$\text{decru}(R_s, R_t) = \begin{cases} (R_s-1, R_t), & R_s \geq R_t, \\ (R_s, R_t-1), & \text{otherwise.} \end{cases}$$

It is coordinatewise nonincreasing, and it is lex-monotone: if $(R_s, R_t) \leq_{\text{lex}} (R'_s, R'_t)$, then either $R_s < R'_s$ (so the first branch cannot produce a larger first coordinate) or $R_s = R'_s$ with $R_t \leq R'_t$, in which case both images either decrement the same coordinate or the smaller pair cannot “overtake” the larger one in lexicographic order.

The map decru from Definition 4 determines how radii shrink once chosen. To make the procedure operative, we also need: (i) an initial choice of radii that guarantees the spheres overlap at the start, and (ii) a way to convert any nonempty overlap into a concrete split point. These are captured by the following two rules.

Definition 5 (Starting rule). A starting rule $\text{staru} : V \times V \rightarrow \mathbb{N}^2$ returns (R_s^0, R_t^0) with nonempty overlap $O(R_s^0, R_t^0) \neq \emptyset$ (e.g., $R_s^0 + R_t^0 \geq d_G(s, t)$; a stronger but safe choice is $S_{R_s^0}(s) \cup S_{R_t^0}(t) = V$).

Definition 6 (Anchor rule). An anchor rule $\text{anru} : \mathcal{P}(V) \rightarrow V$ selects $a \in O(R_s, R_t)$ (e.g., uniform random).

Bringing these pieces together, the three rules: starting rule for initialization (Definition 5), decrement rule for shrinking (Definition 4), and anchor rule for selecting the split point (Definition 6), jointly define the following algorithm, which we refer to as the *Partition cut*:

Algorithm 1 Partition cut

Require: graph $G = (V, E)$, terminals (s, t) , rules $(\text{staru}, \text{decru}, \text{anru})$
Ensure: radii (\bar{R}_s, \bar{R}_t) , overlap O , anchor a

- 1: $(R_s, R_t) \leftarrow \text{staru}(s, t)$
- 2: **while** $O(R_s, R_t) \neq \emptyset$ **do**
- 3: $(\bar{R}_s, \bar{R}_t) \leftarrow (R_s, R_t)$
- 4: $(R_s, R_t) \leftarrow \text{decru}(R_s, R_t)$
- 5: **end while**
- 6: $O \leftarrow O(\bar{R}_s, \bar{R}_t)$, $a \leftarrow \text{anru}(O)$
- 7: **return** $(\bar{R}_s, \bar{R}_t, O, a)$

The intuition behind Algorithm 1 can be explained as follows and is visualized in Figure 2. Grow spheres around s and t until they overlap, then shrink via decru until the next shrink would empty the overlap.

Pick an anchor a according to Definition 6 in this last nonempty overlap, and split the query into $s \rightarrow a$ and $a \rightarrow t$ subproblems on the corresponding induced spheres.

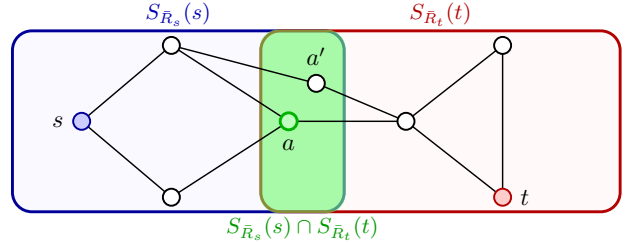


Figure 2: **Last nonempty overlap.** Blue and red spheres overlap in the green region containing both a and a' . Potential anchor node a is selected according to Definition 6.

A natural question is whether the Partition cut of Algorithm 1 actually preserves feasibility of the original $s \rightarrow t$ routing problem. In other words, does splicing the two subpaths at the chosen anchor still yield a valid global route? The following statement makes this precise:

Proposition 4.1 (Feasibility preservation). Let $(\bar{R}_s, \bar{R}_t, O, a)$ be returned by Algorithm 1. If $P_{s \rightarrow a}$ is a feasible path in $G_{\bar{R}_s}^{\text{ind}}(s)$ and $P_{a \rightarrow t}$ is a feasible path in $G_{\bar{R}_t}^{\text{ind}}(t)$, then $P_{s \rightarrow a} \circ P_{a \rightarrow t}$ is a feasible $s \rightarrow t$ path in G .

Proof sketch. Both subgraphs are induced, hence every used edge is in G . Since $a \in O(\bar{R}_s, \bar{R}_t)$, concatenating at a yields a valid $s \rightarrow t$ path in G . \square

4.3 Recursive spherical partitioning

The following algorithm extends the partition cut from Algorithm 1 into a recursive partitioning routine. Its goal is to partition a global $s \rightarrow t$ routing task into a set of smaller subproblems, each confined to an induced sphere whose radius does not exceed a user-defined bound R_{\max} . These subproblems are returned as *task triples* (H, u, w) , meaning: “route from u to w within the induced subgraph H .”

Algorithm 2 starts by initializing the set of tasks \mathcal{T} to be empty (lines 1-3). It then performs a partition cut on the original problem (G, s, t) , which returns the radii (R_s, R_t) , the last nonempty overlap O , and an anchor $a \in O$. The anchor acts as a splitting point that separates the global $s \rightarrow t$ route into two sides.

Algorithm 2 Recursive spherical partitioning

Require: graph $G = (V, E)$, terminals (s, t) ,
 radius cap R_{\max} , rules staru, decru, anru

Ensure: set \mathcal{T} of task triples (H, u, w)

```

1 function SPHPARTITION( $G, s, t, R_{\max}$ )
2    $\mathcal{T} \leftarrow \emptyset$ , rule  $\leftarrow$  (staru, decru, anru)
3    $(R_s, R_t, O, a) \leftarrow \text{PARTCUT}(G, s, t, \text{rule})$      $\triangleright$  Alg. 1
4   if  $R_s \leq R_{\max}$  then
5      $\mathcal{T} \leftarrow \mathcal{T} \cup \{(G_{R_s}^{\text{ind}}(s), s, a)\}$ 
6   else
7      $\mathcal{T} \leftarrow \mathcal{T} \cup \text{SPHPARTITION}(G_{R_s}^{\text{ind}}(s), s, a, R_{\max})$ 
8   end if
9   if  $R_t \leq R_{\max}$  then
10     $\mathcal{T} \leftarrow \mathcal{T} \cup \{(G_{R_t}^{\text{ind}}(t), a, t)\}$ 
11   else
12      $\mathcal{T} \leftarrow \mathcal{T} \cup \text{SPHPARTITION}(G_{R_t}^{\text{ind}}(t), a, t, R_{\max})$ 
13   end if
14   return  $\mathcal{T}$ 
15 end function

```

The algorithm then branches into two recursive checks. On the s -side (lines 4-7), the relevant subproblem is $(G_{R_s}^{\text{ind}}(s), s, a)$. If the radius R_s is already below the cap R_{\max} , this subproblem is considered sufficiently small and is added to the task set \mathcal{T} . If not, the procedure calls itself recursively on this induced subgraph to split it further. Symmetrically, the t -side branch (lines 8-11) processes the subproblem $(G_{R_t}^{\text{ind}}(t), a, t)$: either it is recorded directly if $R_t \leq R_{\max}$, or it is further partitioned by another recursive call.

Finally, once both branches have been processed, the algorithm returns (line 12) the accumulated set \mathcal{T} of task triples. By construction, concatenating the solutions to these recorded subproblems along their anchors yields a valid overall $s \rightarrow t$ route.

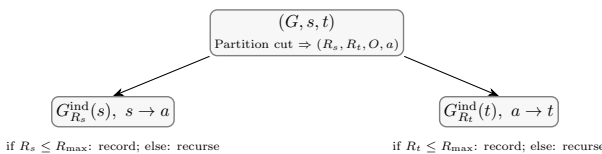


Figure 3: **Recursive splitting.** Any side above the radius cap is split again by Algorithm 1; leaves are independent subproblems.

Figure 3 illustrates this recursive structure. Each partition cut splits the problem into two boxes, one for the start-side and one for the target-side. If the radius on a side is within the threshold, the box is recorded as a leaf; otherwise, it is expanded by another partition cut.

4.3.1 Baseline application

The recursive partition in Algorithm 2 produces a set of leaf tasks, each represented by a triple (H, u, w) where H is an induced spherical subgraph and u, w are its boundary terminals. At this stage, the global $s \rightarrow t$ routing problem has been reduced to a collection of independent local subproblems, each small enough to be solved efficiently by standard methods.

Algorithm 3 Baseline application with spherical partitioning

Require: graph $G = (V, E)$, terminals (s, t) ,
 radius cap R_{\max} , solver $\text{optimize}(\cdot)$

Ensure: feasible route \mathcal{R}

```

1:  $\mathcal{R} \leftarrow \emptyset$ ;  $\mathcal{T} \leftarrow \text{SPHPARTITION}(G, s, t, R_{\max})$ 
2: for all  $(H, u, w) \in \mathcal{T}$  do
3:    $\mathcal{R} \leftarrow \mathcal{R} \circ \text{optimize}(H, u, w)$ 
4: end for
5: return  $\mathcal{R}$ 

```

Algorithm 3 describes how to turn the recursive spherical partitioning into a full routing solution. First, the input graph G with terminals s, t is partitioned into a collection of smaller subproblems (line 3). Each subproblem (H, u, w) is an induced subgraph H together with its local terminals u and w . Then, for each subproblem, an arbitrary downstream solver $\text{optimize}(H, u, w)$ is applied to compute a local path (lines 4-5). These local solutions are concatenated in the order determined by the anchors of the partition, resulting in a valid global route \mathcal{R} from s to t (line 6). Since the subproblems are independent, they can also be solved in parallel, and the procedure remains agnostic to the choice of solver.

5 Numerical Experiments

Our experiments are designed to evaluate whether our method delivers significant performance gains (in terms of runtime and optimality gap) over established graph-routing baselines.

5.1 Dataset

For our empirical evaluation we use the well-known **West-USA-road** benchmark suite from the 9th DIMACS Implementation Challenge on Shortest Paths (DIM, 2006). These graphs encode real-world road networks at the level of individual intersections and

road segments. Each node corresponds to a road intersection or endpoint, and each edge represents a street segment with a positive weight equal to its physical length. The dataset is widely used in the routing literature as a benchmark for large-scale shortest-path computations, since it combines realistic geometry, heterogeneous edge weights, and large graph sizes (millions of nodes and edges).

5.2 Experimental setup

For each problem seed $p \in \{1, \dots, 30\}$ we draw a source-target pair (s, t) uniformly at random from the node set (rejecting $s = t$). For each (s, t) , we run five independent trials with inner seeds $q \in \{1, \dots, 5\}$ to capture variability from randomized components. For instance, the anchors are selected randomly according to Definition 6. We report results per instance and aggregate by averaging across the 5 inner seeds for each problem seed.

Given (s, t) , we apply Algorithm 2 and selects an anchor node uniformly at random from this set of nodes (the randomness is controlled by the inner seed q). The graph is partitioned into subgraphs around s and t until a maximum radius threshold is met. R_{\max} from Algorithm 3 is set to 1800. Throughout development we found a robust rule of thumb: when routing within a spherical subgraph of hop radius R , choosing $R_{\max} \in [R/2, R/1.7]$ delivers high-quality solutions at both low computational cost and effort. For the West-USA instances, a single sphere with $R \approx 3200$ covers the region; thus $R_{\max} = 1800$ lies squarely in this band, balancing overlap likelihood and leaf size. Each subgraph shortest-path subproblem is solved with Dijkstra's algorithm. Because our spherical partitioning produces independent induced subgraphs, we parallelize these subgraph solves and report end-to-end wall-clock time (including partition cut and final concatenation). By contrast, the baselines do not naturally partition into independent leaf tasks so we do not apply the same solving subproblem parallelization to them.

Baselines. As baselines, we first include an optimal reference obtained by running Dijkstra's algorithm directly on the full graph. To compare against partition-based approaches, we also evaluate a corridor-routing strategy in which the graph is partitioned into $k = 64$ cells using PyMetis; a path is computed on the resulting *quotient graph*, and Dijkstra's algorithm is then applied within the induced corridor to recover a detailed route (Karypis

and Kumar, 1998). In addition, we test a partition heuristic based on community detection via the Louvain method: routing is first performed on the community graph, and the solution is subsequently refined by applying Dijkstra on the induced subgraph spanned by the relevant communities (default parameters; seeded where applicable) (Blondel et al., 2008). The corridor-routing and Louvain pipelines introduce partitions, yet can not be solved independently and not conditioned on the specific (s, t) , so they likewise do not yield independent leaves that one could solve with a plug-in solver and then concatenate repair-free (e.g. fixing feasibility) (Karypis and Kumar, 1998; Blondel et al., 2008).

Metrics. Let $m \in \{\text{SPHERE, CORRIDOR, LOUVAIN}\}$ denote the method. For each problem seed p and inner seed q , let $C_{p,q}^{(m)}$ be the route cost returned by m , and let C_p^* be the shortest-path cost from Dijkstra's algorithm on the full graph for the same (s, t) . Define the relative optimality gap

$$\Delta_{p,q}^{(m)} = \frac{C_{p,q}^{(m)} - C_p^*}{C_p^*}.$$

For each p , aggregate across the five inner seeds by the median:

$$\tilde{\Delta}_p^{(m)} = \text{median}_{q=1,\dots,5} \Delta_{p,q}^{(m)},$$

$$\tilde{T}_p^{(m)} = \text{median}_{q=1,\dots,5} T_{p,q}^{(m)},$$

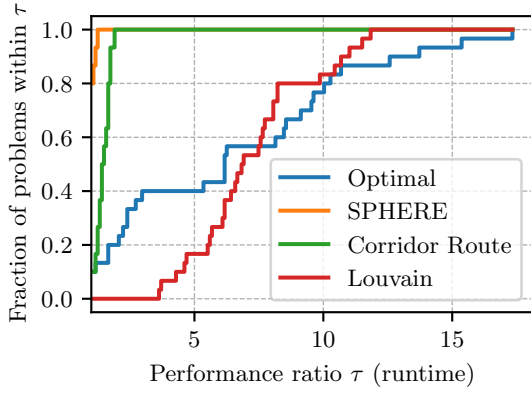
where $T_{p,q}^{(m)}$ is the end-to-end wall-clock time. For completeness, we also report means:

$$\bar{\Delta}_p^{(m)} = \frac{1}{5} \sum_{q=1}^5 \Delta_{p,q}^{(m)}, \quad \bar{T}_p^{(m)} = \frac{1}{5} \sum_{q=1}^5 T_{p,q}^{(m)}.$$

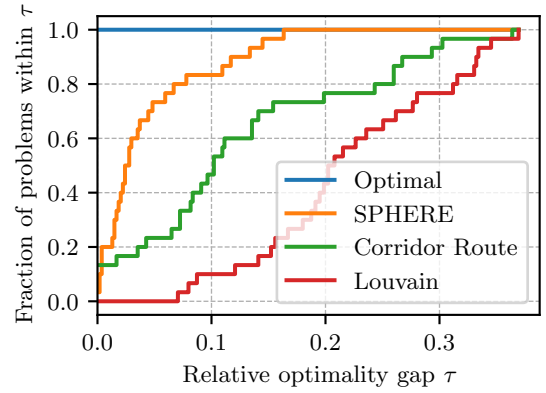
5.3 Results

Across 30 West-USA instances with five inner seeds each, SPHERE achieves faster end-to-end runtimes than the three baselines and matches near-optimal route quality. We use performance and accuracy profiles for visualization (Dolan and Moré, 2002; Beiranvand et al., 2017). Both are computed per instance from the median over seeds. Mean-based profiles for runtime and accuracy are presented as well.

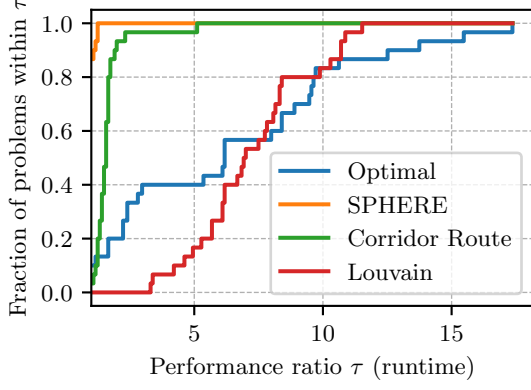
Runtime. Figures 4a and 4c plot the fraction of instances solved within a performance ratio τ of the best method on that instance. SPHERE's curve lies above the Louvain and corridor routes for most



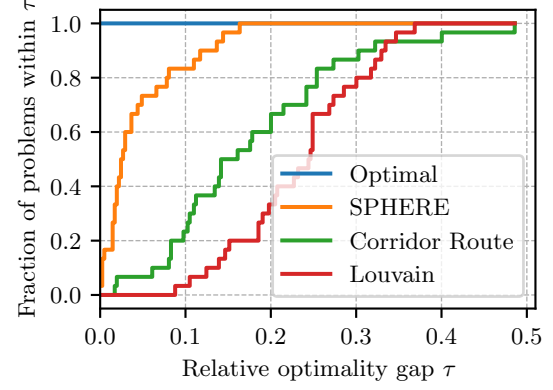
(a) Runtime profile based on the **median** over five seeds



(b) Accuracy profile based on the **median** over five seeds



(c) Runtime profile based on the **mean** over five seeds



(d) Accuracy profile based on the **mean** over five seeds

Figure 4: Performance and accuracy profiles of 30 instances based on median and mean over five seeds.

τ , indicating uniformly stronger or equal runtime across instances. Interestingly, for small τ , Louvain’s curve lies below Dijkstra’s, despite being a suboptimal method. However, at larger τ it crosses and stays above, indicating tail slowdowns for Dijkstra. This suggests that SPHERE not only improves median runtime, but also avoids the heavy-tailed slowdowns observed in both Dijkstra and Louvain, resulting in tighter runtime distributions and fewer extreme outliers, which makes SPHERE’s runtimes more predictable across different instances.

Route quality. Figures 4b and 4d reports the fraction of instances whose relative optimality gap is at most τ . Dijkstra attains zero gap by construction. SPHERE’s curve dominates the partition baselines across τ , yielding smaller or equal gaps on the majority of instances. This confirms that cutting inside the s - t overlap and solving on induced spheres pre-

serves high-quality routes without boundary repair.

Pareto dominance Against the partition baselines (Louvain and METIS corridor), SPHERE Pareto-dominates on 26 of 30 instances in terms of average metrics. It is both faster and has a smaller optimality gap (Appendix A.3). The remaining three show a speed-quality trade-off where SPHERE is not dominated by another algorithm. In other words, SPHERE consistently lies on or close to the empirical speed-quality frontier, while Louvain and corridor-routing often face a trade-off between being faster but less accurate, or more accurate but substantially slower.

Robustness and aggregation Repeating the analysis with means over seeds yields profiles that do not differ materially from the median-based plots, supporting robustness to the randomized anchor se-

lection. Additionally, the full results in the appendix show low dispersion across seeds. For SPHERE, the optimality-gap standard deviation is 0 on 16 instances and is the lowest among all methods on all but one instance. For further Information, we refer to Appendix A.3.

6 Conclusion and Outlook

We introduced SPHERE, a routing scheme that splits an $s-t$ query by cutting *inside* the last nonempty overlap of hop-spheres around s and t . This placement preserves feasibility without boundary repair, confines each side to an induced subgraph, and allows the two subproblems to be solved independently with standard shortest-path routines and in parallel.

On **West-USA-road** graphs, SPHERE achieves faster end-to-end times and equal or smaller optimality gaps than a Louvain-based route and a METIS-corridor pipeline on the large majority of instances; runtimes are also more predictable, as heavy-tail slowdowns seen for the baselines largely disappear. In contrast to bidirectional search, which still explores a single coupled state space, SPHERE yields separable leaves. In contrast to static partitions whose cuts ignore (s, t) and can sever bottlenecks, cutting within the overlap keeps the route intact and avoids corridor repair.

Looking ahead, the main levers are the *starting rule*, the *decrement rule*, and the *anchor selection*. Even simple choices already perform well, but data-driven or adaptive variants should improve robustness across graphs and query distributions. A second priority is to tune the radius cap R_{\max} automatically (per instance or region) to balance overlap likelihood against subproblem size. These steps retain the current simplicity and parallelism while targeting further speed and stability.

References

The shortest path problem: Ninth dimacs implementation challenge. volume 74 of *DIMACS Series in Discrete Mathematics and Theoretical Computer Science*. American Mathematical Society, 2006.

Ittai Abraham, Daniel Delling, Andrew V Goldberg, and Renato F Werneck. A hub-based labeling algorithm for shortest paths in road networks. In *International Symposium on Experimental Algorithms*, pages 230–241. Springer, 2011.

Hannah Bast, Daniel Delling, Andrew Goldberg, Matthias Müller-Hannemann, Thomas Pajor, Peter Sanders, Dorothea Wagner, and Renato F Werneck. Route planning in transportation networks. In *Algorithm engineering: Selected results and surveys*, pages 19–80. Springer, 2016.

Vahid Beiranvand, Warren Hare, and Yves Lucet. Best practices for comparing optimization algorithms. *Optimization and Engineering*, 18(4):815–848, 2017.

Vincent D. Blondel, Jean-Loup Guillaume, Renaud Lambiotte, and Etienne Lefebvre. Fast unfolding of communities in large networks. *Journal of Statistical Mechanics: Theory and Experiment*, (10):P10008, 2008. doi: 10.1088/1742-5468/2008/10/P10008.

Edsger W. Dijkstra. A note on two problems in connexion with graphs. *Numerische Mathematik*, 1: 269–271, 1959. doi: 10.1007/BF01386390.

Elizabeth D Dolan and Jorge J Moré. Benchmarking optimization software with performance profiles. *Mathematical programming*, 91(2):201–213, 2002.

Dominique Feillet, Pierre Dejax, and Michel Gendreau. An exact algorithm for the elementary shortest path problem with resource constraints: Application to some vehicle routing problems. *Networks*, 44(3):190–204, 2004. doi: 10.1002/net.20033.

Robert Geisberger, Peter Sanders, Dominik Schultes, and Daniel Delling. Contraction hierarchies: Faster and simpler hierarchical routing in road networks. In *International workshop on experimental and efficient algorithms*, pages 319–333. Springer, 2008.

Andrew V Goldberg and Chris Harrelson. Computing the shortest path: A search meets graph theory. In *SODA*, volume 5, pages 156–165, 2005.

Ron Gutman. Reach-based routing: A new approach to shortest path algorithms optimized for road net-

works. In *Proceedings of the Sixth Workshop on Algorithm Engineering and Experiments and the First Workshop on Analytic Algorithms and Combinatorics*, pages 100–111, 2004.

Peter E Hart, Nils J Nilsson, and Bertram Raphael. A formal basis for the heuristic determination of minimum cost paths. *IEEE transactions on Systems Science and Cybernetics*, 4(2):100–107, 1968.

Refael Hassin. Approximation schemes for the restricted shortest path problem. *Mathematics of Operations Research*, 17(1):36–42, 1992. doi: 10.1287/moor.17.1.36.

Robert C. Holte, Ariel Felner, Guni Sharon, and Nathan R. Sturtevant. Bidirectional search that is guaranteed to meet in the middle. In *Proceedings of the Thirtieth AAAI Conference on Artificial Intelligence (AAAI-16)*, pages 3411–3417. AAAI Press, 2016. URL <https://ojs.aaai.org/index.php/AAAI/article/view/10251>.

Stefan Irnich and Guy Desaulniers. Shortest path problems with resource constraints. In Guy Desaulniers, Jacques Desrosiers, and Marius M. Solomon, editors, *Column Generation*, pages 33–65. Springer, Boston, MA, 2005. doi: 10.1007/0-387-25486-2_2.

Hermann Kaindl and Gerhard Kainz. Bidirectional heuristic search reconsidered. *Journal of Artificial Intelligence Research*, 7:283–317, 1997. doi: 10.1613/jair.387.

George Karypis and Vipin Kumar. A fast and high quality multilevel scheme for partitioning irregular graphs. *SIAM Journal on Scientific Computing*, 20(1):359–392, 1998. doi: 10.1137/S1064827595287997.

Brian W. Kernighan and Shen Lin. An efficient heuristic procedure for partitioning graphs. *The Bell System Technical Journal*, 49(2):291–307, 1970. doi: 10.1002/j.1538-7305.1970.tb01770.x.

T. A. J. Nicholson. Finding the shortest route between two points in a network. *The Computer Journal*, 9(3):275–280, 1966. doi: 10.1093/comjnl/9.3.275.

David Pisinger and Stefan Ropke. A general heuristic for vehicle routing problems. *Computers & Operations Research*, 34(8):2403–2435, 2007. doi: 10.1016/j.cor.2005.09.012.

Ira Pohl. Bi-directional and heuristic search in path problems. Technical Report SLAC-104, Stanford Linear Accelerator Center, Stanford, CA, 1969. URL <https://www.slac.stanford.edu/pubs/slacpubs/00150/slac-pub-0104.pdf>.

Jianbo Shi and Jitendra Malik. Normalized cuts and image segmentation. *IEEE Transactions on Pattern Analysis and Machine Intelligence*, 22(8):888–905, 2000. doi: 10.1109/34.868688.

Thibaut Vidal. Hybrid genetic search for the cvrp: Open-source implementation and swap* neighborhood. *Computers & Operations Research*, 140:105564, 2022. doi: 10.1016/j.cor.2021.105564.

A Appendix

A.1 Notation

Table 1: Notation

Symbol	Description
$V = \{1, \dots, m\}$	Node (vertex) index set.
$\mathcal{P}(V)$	Power set of V .
$E \subseteq V \times V$	Edge set; undirected unless stated.
$G = (V, E)$	Graph with node set V and edge set E .
$d_G(u, v)$	Shortest unweighted path distance on G .
$G[U]$	Induced subgraph on node set U .
$S_R(\tilde{v}) = \{v \in V : d_G(\tilde{v}, v) \leq R\}$	(Closed) hop sphere (ball) of radius R around \tilde{v} .
$S_s(r) \equiv S_r(s)$, $S_t(r) \equiv S_r(t)$	Shorthand spheres around s and t .
$O(R_s, R_t) = S_{R_s}(s) \cap S_{R_t}(t)$	Overlap of the two spheres.
$a \in V$, $S^\dagger \subseteq O(R_s, R_t)$	Anchor node; optional candidate anchor set.
$G_s = G[S_{R_s}(s)]$, $G_t = G[S_{R_t}(t)]$	Induced subgraphs around s and t at radii R_s, R_t .

Continued on next page

Table 1: Notation (Continued)

Symbol	Description
$V = \{1, \dots, m\}$	Node (vertex) index set.
$(H, u, w), \mathcal{T}$	Task triple “route $u \rightarrow w$ inside H ”; set of leaf tasks.
$ X $	Cardinality of a (finite) set X .

A.2 Parameters

Table 2: Parameters

Symbol	Description
$R_{\max} \in \mathbb{N}$	Maximum allowed radius for spherical subgraphs (controls subproblem diameter).
$V_{\max} \in \mathbb{N}, E_{\max} \in \mathbb{N}$	Optional caps on nodes/edges permitted in any subgraph $G[U]$.
$\varepsilon_{\text{overlap}} \in \mathbb{N}_0$	Minimum required overlap size (require $ O(R_s, R_t) \geq \varepsilon_{\text{overlap}}$).
$\Delta r \in \mathbb{N}$	Radius increment/decrement step during sphere growth/shrinking (if using fixed steps; typically $\Delta r = 1$).
$L_{\max} \in \mathbb{N}$	Maximum recursion depth for repeated splits.
$k_{\text{anchor}} \in \mathbb{N}$	Number of anchors to select from O (often $k_{\text{anchor}} = 1$).

A.3 Performance per instance

Table 3: WestUSA – Routing

		avg compute time	avg opt. gap	median opt. gap	std opt. gap
P1	SPHERE	135.73	0.08	0.06	0.02
	Corridor Route	173.97	0.24	0.07	0.36
P2	Louvain	1047.77	0.25	0.28	0.05
	SPHERE	138.27	0.12	0.12	0.00
P3	Corridor Route	187.87	0.14	0.09	0.16
	Louvain	1072.17	0.34	0.35	0.05
P4	SPHERE	165.25	0.03	0.03	0.00
	Corridor Route	190.12	0.08	0.10	0.06
P5	Louvain	1130.18	0.18	0.18	0.05
	SPHERE	370.06	0.11	0.11	0.00
P6	Corridor Route	574.18	0.25	0.26	0.10
	Louvain	1230.71	0.37	0.37	0.03
P7	SPHERE	126.88	0.05	0.05	0.00
	Corridor Route	171.35	0.10	0.11	0.06
P8	Louvain	1129.89	0.14	0.14	0.06
	SPHERE	301.07	0.02	0.03	0.00
P9	Corridor Route	571.56	0.18	0.15	0.14
	Louvain	1265.49	0.25	0.20	0.12
P10	SPHERE	213.59	0.00	0.00	0.00
	Corridor Route	354.04	0.27	0.36	0.17
P11	Louvain	1197.91	0.32	0.32	0.04
	SPHERE	157.02	0.01	0.01	0.00
P12	Corridor Route	224.89	0.32	0.27	0.16
	Louvain	1165.53	0.09	0.07	0.03
P13	SPHERE	390.68	0.02	0.02	0.00
	Corridor Route	396.99	0.13	0.10	0.10
P14	Louvain	1274.68	0.23	0.21	0.06
	SPHERE	137.20	0.02	0.02	0.00
P15	Corridor Route	197.31	0.02	0.00	0.03
	Louvain	1141.72	0.27	0.33	0.10
P16	SPHERE	130.96	0.13	0.13	0.01
	Corridor Route	167.76	0.20	0.07	0.24
P17	Louvain	1057.36	0.33	0.33	0.00
	SPHERE	264.38	0.04	0.04	0.00
P18	Corridor Route	234.53	0.24	0.20	0.13
	Louvain	1160.17	0.25	0.17	0.13
P19	SPHERE	123.22	0.00	0.00	0.00
	Corridor Route	200.92	0.10	0.00	0.16
P20	Louvain	1308.92	0.18	0.19	0.03
	SPHERE	234.34	0.14	0.14	0.00
P21	Corridor Route	358.43	0.25	0.24	0.17
	Louvain	1414.78	0.33	0.31	0.05

Continued on next page

		avg compute time	avg opt. gap	median opt. gap	std opt. gap
P15	SPHERE	211.37	0.00	0.00	0.00
	Corridor Route	300.88	0.11	0.10	0.09
	Louvain	1288.33	0.15	0.15	0.02
P16	SPHERE	136.40	0.04	0.04	0.00
	Corridor Route	221.84	0.08	0.02	0.13
	Louvain	1400.16	0.20	0.19	0.05
P17	SPHERE	119.90	0.01	0.00	0.02
	Corridor Route	193.90	0.02	0.00	0.03
	Louvain	1266.58	0.20	0.21	0.07
P18	SPHERE	123.18	0.08	0.08	0.01
	Corridor Route	205.16	0.06	0.00	0.07
	Louvain	1409.96	0.32	0.33	0.03
P19	SPHERE	205.97	0.02	0.02	0.00
	Corridor Route	1052.15	0.40	0.30	0.31
	Louvain	1401.55	0.25	0.25	0.05
P20	SPHERE	170.12	0.00	0.00	0.00
	Corridor Route	391.16	0.30	0.08	0.34
	Louvain	1414.17	0.10	0.08	0.04
P21	SPHERE	326.25	0.01	0.01	0.00
	Corridor Route	506.65	0.20	0.14	0.12
	Louvain	1502.53	0.30	0.22	0.16
P22	SPHERE	137.27	0.03	0.03	0.00
	Corridor Route	180.60	0.49	0.29	0.51
	Louvain	1135.72	0.28	0.26	0.08
P23	SPHERE	172.50	0.01	0.01	0.00
	Corridor Route	211.28	0.08	0.04	0.11
	Louvain	1065.85	0.21	0.20	0.06
P24	SPHERE	145.29	0.02	0.02	0.00
	Corridor Route	202.11	0.21	0.26	0.13
	Louvain	1009.77	0.27	0.28	0.07
P25	SPHERE	160.44	0.02	0.02	0.00
	Corridor Route	219.89	0.11	0.04	0.14
	Louvain	1059.09	0.12	0.12	0.02
P26	SPHERE	172.71	0.03	0.03	0.00
	Corridor Route	203.42	0.17	0.13	0.14
	Louvain	1054.63	0.24	0.19	0.13
P27	SPHERE	246.94	0.02	0.02	0.00
	Corridor Route	479.93	0.14	0.06	0.11
	Louvain	1388.28	0.22	0.20	0.04
P28	SPHERE	159.42	0.00	0.00	0.00
	Corridor Route	267.58	0.16	0.13	0.17
	Louvain	1274.86	0.19	0.16	0.08

Continued on next page

		avg compute time	avg opt. gap	median opt. gap	std opt. gap
P29	SPHERE	232.46	0.07	0.07	0.00
	Corridor Route	354.39	0.14	0.11	0.07
	Louvain	1219.90	0.25	0.24	0.03
P30	SPHERE	142.64	0.16	0.16	0.00
	Corridor Route	175.93	0.10	0.08	0.10
	Louvain	1162.54	0.15	0.09	0.10
